



THE UNIVERSITY *of* EDINBURGH

## Edinburgh Research Explorer

# 11-hydroxysteroid dehydrogenase type 2 deficiency accelerates atherogenesis and causes proinflammatory changes in the endothelium in apoe<sup>-/-</sup> mice

### Citation for published version:

Deuchar, GA, McLean, D, Hadoke, PWF, Brownstein, DG, Webb, DJ, Mullins, JJ, Chapman, K, Seckl, JR & Kotelevtsev, YV 2011, '11-hydroxysteroid dehydrogenase type 2 deficiency accelerates atherogenesis and causes proinflammatory changes in the endothelium in apoe<sup>-/-</sup> mice', *Endocrinology*, vol. 152, no. 1, pp. 236-246. <https://doi.org/10.1210/en.2010-0925>

### Digital Object Identifier (DOI):

[10.1210/en.2010-0925](https://doi.org/10.1210/en.2010-0925)

### Link:

[Link to publication record in Edinburgh Research Explorer](#)

### Document Version:

Publisher's PDF, also known as Version of record

### Published In:

Endocrinology

### Publisher Rights Statement:

© 2011 by The Endocrine Society

### General rights

Copyright for the publications made accessible via the Edinburgh Research Explorer is retained by the author(s) and / or other copyright owners and it is a condition of accessing these publications that users recognise and abide by the legal requirements associated with these rights.

### Take down policy

The University of Edinburgh has made every reasonable effort to ensure that Edinburgh Research Explorer content complies with UK legislation. If you believe that the public display of this file breaches copyright please contact [openaccess@ed.ac.uk](mailto:openaccess@ed.ac.uk) providing details, and we will remove access to the work immediately and investigate your claim.



## 11 $\beta$ -Hydroxysteroid Dehydrogenase Type 2 Deficiency Accelerates Atherogenesis and Causes Proinflammatory Changes in the Endothelium in *ApoE*<sup>-/-</sup> Mice

Graeme A. Deuchar,\* Danielle McLean,\* Patrick W. F. Hadoke, David G. Brownstein, David J. Webb, John J. Mullins, Karen Chapman, Jonathan R. Seckl, and Yuri V. Kotelevtsev

Centre for Cardiovascular Science (G.A.D., D.M., P.W.F.H., D.G.B., D.J.W., J.J.M., K.C., J.R.S.), The Queen's Medical Research Institute, College of Medicine and Veterinary Medicine, University of Edinburgh, Edinburgh EH16 4TJ, United Kingdom; and Puschino State University (Y.V.K.), 142292 Russia, Puschino, Moscow Region

Mineralocorticoid receptor (MR) activation is proinflammatory and proatherogenic. Antagonism of MR improves survival in humans with congestive heart failure caused by atherosclerotic disease. In animal models, activation of MR exacerbates atherosclerosis. The enzyme 11 $\beta$ -hydroxysteroid dehydrogenase type 2 (11 $\beta$ -HSD2) prevents inappropriate activation of the MR by inactivating glucocorticoids in mineralocorticoid-target tissues. To determine whether glucocorticoid-mediated activation of MR increases atheromatous plaque formation, we generated *ApoE*<sup>-/-</sup>/11 $\beta$ -HSD2<sup>-/-</sup> double-knockout (*E/b2*) mice. On chow diet, *E/b2* mice developed atherosclerotic lesions by 3 months of age, whereas Apolipoprotein E (*ApoE*<sup>-/-</sup>) mice remained lesion free. Brachiocephalic plaques in 3-month-old *E/b2* mice showed increased macrophage and lipid content and reduced collagen content compared with similar sized brachiocephalic plaques in 6-month-old *ApoE*<sup>-/-</sup> mice. Crucially, treatment of *E/b2* mice with eplerenone, an MR antagonist, reduced plaque development and macrophage infiltration while increasing collagen and smooth muscle cell content without any effect on systolic blood pressure. In contrast, reduction of systolic blood pressure in *E/b2* mice using the epithelial sodium channel blocker amiloride produced a less-profound atheroprotective effect. Vascular cell adhesion molecule 1 expression was increased in the endothelium of *E/b2* mice compared with *ApoE*<sup>-/-</sup> mice. Similarly, aldosterone increased vascular cell adhesion molecule 1 expression in mouse aortic endothelial cells, an effect mimicked by corticosterone only in the presence of an 11 $\beta$ -HSD2 inhibitor. Thus, loss of 11 $\beta$ -HSD2 leads to striking atherogenesis associated with activation of MR, stimulating proinflammatory processes in the endothelium of *E/b2* mice. (*Endocrinology* 152: 236–246, 2011)

**A**therosclerosis is a chronic inflammatory response to injury in the vessel wall, yet the initiating events that precede leukocyte accumulation and fat deposition leading to plaque development remain poorly defined. Mineralocorticoid receptor (MR) antagonists, administered as diuretics at doses that do not significantly lower blood pressure, improve survival in heart failure (1), and acute myocardial infarction (2) in humans. Activation of MR in the vasculature is also proinflammatory and proathero-

genic (3), suggesting protective effects of MR antagonism on the cardiovascular system, independent of blood pressure. However, the mechanisms associated with these cardio-protective effects in humans are yet to be determined. MR are also high affinity glucocorticoid receptors (4), yet in mineralocorticoid target tissues, including the distal nephron, MR are selective for aldosterone, their physiological ligand, despite higher (~100-fold) circulating levels of glucocorticoid (5). This selectivity at least in part is

ISSN Print 0013-7227 ISSN Online 1945-7170

Printed in U.S.A.

Copyright © 2011 by The Endocrine Society

doi: 10.1210/en.2010-0925 Received August 13, 2010. Accepted October 18, 2010.

First Published Online November 24, 2010

\* G.A.D. and D.M. contributed equally to this work.

Abbreviations: ApoE, Apolipoprotein E; *E/b2*, *ApoE*<sup>-/-</sup>/*Hsd11b2*<sup>-/-</sup> double-knockout; ENaC, epithelial sodium channel; 11 $\beta$ -HSD2, 11 $\beta$ -hydroxysteroid dehydrogenase type 2; MAEC, mouse aortic endothelial cell; MR, mineralocorticoid receptor; SBP, systolic blood pressure; SMA, smooth muscle actin; SMC, smooth muscle cell; UST, United States trichrome; VCAM-1, vascular cell adhesion molecule 1.

a consequence of prereceptor metabolism of glucocorticoids to intrinsically inert 11-keto-glucocorticoids by 11 $\beta$ -hydroxysteroid dehydrogenase type 2 (11 $\beta$ -HSD2) (6). The pathophysiological importance of 11 $\beta$ -HSD2 is demonstrated in patients with the syndrome of apparent mineralocorticoid excess caused by mutations in *Hsd11b2*, the human gene encoding 11 $\beta$ -HSD2 (7). Loss of 11 $\beta$ -HSD2 results in inappropriate activation of MR by glucocorticoids in the distal nephron causing hypokalemia and hypertension (8). Similarly, 11 $\beta$ -HSD2<sup>-/-</sup> mice are also hypertensive, with activation of MR in the distal nephron causing increased sodium reabsorption and potassium excretion (9).

Evidence supports a proatherogenic action of cortisol within the vessel wall (10). Glucocorticoid pharmacotherapy in humans is associated with increased cardiovascular events (11).

We and others have demonstrated the existence of the MR/11 $\beta$ -HSD2 system in nonepithelial tissues, including the vasculature (12). Thus, proatherogenic effects of MR activation could be mediated directly by increased mineralocorticoid hormones or through by-pass or reduced activity of vascular 11 $\beta$ -HSD2, permitting glucocorticoid activation of vascular MR. All known inhibitors of 11 $\beta$ -HSD2 can also inhibit 11 $\beta$ -HSD1 activity (13) and compromise the endothelial barrier by interacting with tight junction proteins (14). Therefore, we have investigated the underlying mechanism in *Apoe*<sup>-/-</sup>/*Hsd11b2*<sup>-/-</sup> double-knockout (E/b2) mice, lacking both apolipoprotein E (ApoE) and 11 $\beta$ -HSD2.

## Materials and Methods

### Generation of ApoE/Hsd11b2 double-knockout animals

All animal studies were conducted in accordance with the National Institutes of Health guidelines for the Care and Use of Laboratory Animals under the auspices of the Animals (Scientific Procedures) Act UK 1986 after prior approval by the local ethical committee. The previously targeted *Hsd11b2* allele (9) was transferred to C57BL/6J by nine generations of consecutive backcrosses. Two C57BL/6J females homozygous for deletion of the *Hsd11b2* allele were crossed with an *Apoe*-knockout (*Apoe*<sup>-/-</sup>) male on the C57BL/6J background (Charles River, L'Arbresles Cedex, France) derived from the original knockout line (15). Double heterozygous male offspring (*Apoe*<sup>+/-</sup>/*Hsd11b2*<sup>+/-</sup>) were backcrossed to *Apoe*<sup>-/-</sup> females; progeny was subsequently intercrossed to produce double homozygous knockout animals (*Apoe*<sup>-/-</sup>/*Hsd11b2*<sup>-/-</sup>). The colony was maintained by crossing homozygous *Apoe*<sup>-/-</sup>/*Hsd11b2*<sup>-/-</sup> knockout males (E/b2) to *Apoe*<sup>-/-</sup>/*Hsd11b2*<sup>+/-</sup> females; double-knockout E/b2 progeny was selected for experimental protocols. Genotyping was performed by PCR using genomic DNA extracted from ear clips. *Apoe* primers were located outside the neocassette inserted into exons 3 and 4 (ApoEex3f, AAC TTA CTC TAC ACA GGA TGC C; *Apoe*

ex4r, CGT CAT AGT GTC CTC CAT CAG TGC). These primers amplify both the wild-type allele (584 bp) and the knockout allele (1500 bp). PCR conditions were as follows: denaturation at 94 C for 5 min, then 3 min of elongation at 72 C, followed by 32 cycles of 94 C for 30 sec, 58 C for 1 min, and 72 C for 2 min. The *Hsd11b2* allele (981 bp) was amplified with primers 11b2\_679f, AGG CTG ATG ATA GAT TCA CGA GAC; and 11b2\_1660r, CGA ATG TGT CCA TAA GCA GTG. The knockout allele was amplified using the genomic primer 11b2\_679f (above) and primer Neof1441, GCG AAT GGG CTG ACC GCT TCC TCG, complementary to the Neo gene sequence in the targeting cassette inserted in the reverse orientation.

### Animal treatments

Male *Apoe*<sup>-/-</sup> and E/b2 mice were maintained on normal chow diet with water *ad libitum* and a 12-h light, 12-h dark cycle. Systolic blood pressure (SBP) was measured in conscious, restrained mice by noninvasive tail cuff plethysmography (16). This procedure was repeated on a weekly basis during the first month followed by monthly measurements until termination. Representative *Apoe*<sup>-/-</sup> and E/b2 mice were killed by asphyxiation with CO<sub>2</sub> at age 3 and 6 months for assessment of atherosclerotic lesion formation. To evaluate the effects of drugs, 2-month-old male E/b2 and *Apoe*<sup>-/-</sup> mice were randomized to receive normal chow diet containing the MR antagonist eplerenone (200 mg/kg · d), the epithelial sodium channel (ENaC) blocker amiloride (1 mg/kg · d; n = 9) that acts downstream of renal MR to lower blood pressure (17), or vehicle for 3 months.

### Tissue preparation for assessment of atherosclerosis

After euthanasia, the vasculature was perfusion fixed *in situ* with 10% neutral-buffered paraformaldehyde via the left ventricle. Arteries removed included the aorta and the following major branches: brachiocephalic (innominate) artery and its branches, the right subclavian and right common carotid arteries, the left common carotid and left subclavian arteries, and the major branches of the abdominal aorta, including the celiac, superior mesenteric arteries, and the renal arteries.

### Semiquantitative gross assessment of atherosclerosis in the arterial tree

Adventitia were dissected from fixed arteries under a dissecting microscope. Atherosclerotic lesions were visualized through the translucent arterial wall as yellowish-white opaque deposits. A semiquantitative scoring system was applied for atherosclerotic deposits at the following sites: 1) lesser curvature of the aortic arch, 2) origins of principal branches of thoracic aorta (brachiocephalic, left common carotid, and left subclavian arteries), 3) origin of right and distal right and left common carotid arteries, 4) distal right and left subclavian arteries, and 5) principal branches of abdominal aorta (celiac, superior mesenteric, and renal arteries). Scoring was based on the following criteria: 0, absent; 1, trace; 2, mild; 3, moderate; and 4, severe.

Arterial trees from all mice of both genotypes were coded and read blind by two independent observers. For each site, the arterial tree with the most severe deposit was assigned a score of 4. The remaining coded arterial trees were then assigned a score based on that sample.

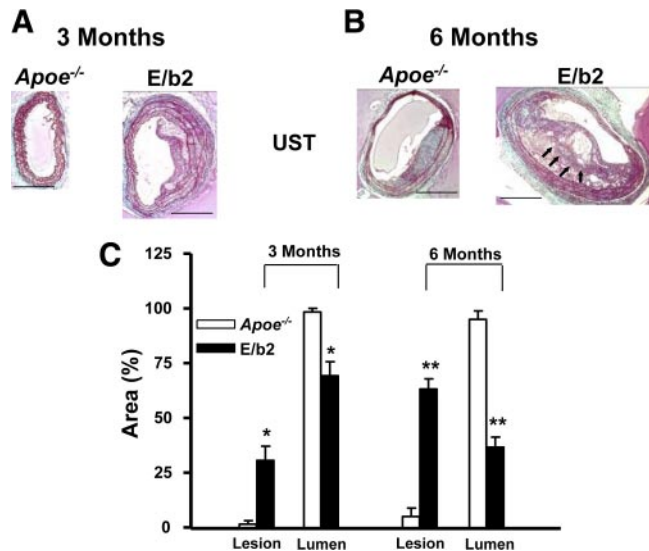


**FIG. 1.** Accelerated atherosclerosis in *Apoe*<sup>-/-</sup> mice on a standard low-fat diet. **A**, Atherosclerotic lesions and outward remodeling were evident in the brachiocephalic arteries of 3-month-old *E/b2* mice but not in *Apoe*<sup>-/-</sup> mice (UST stain; magnification,  $\times 10$ ). **B**, At 6 months of age, lesion development and outward remodeling were significantly greater in *E/b2* than in *Apoe*<sup>-/-</sup> mice. The example used for *Apoe*<sup>-/-</sup> shows the largest plaque seen at this age (UST stain; magnification,  $\times 10$ ). Lesions in *E/b2* were more complex with evidence of buried fibrous caps (black arrows). Scale bar, 250  $\mu\text{m}$ . **C**, Quantitative analysis confirmed that lesion sizes were increased, and lumens were reduced in *E/b2* mice compared with *Apoe*<sup>-/-</sup> mice. Data are means  $\pm$  SEM; \*,  $P < 0.05$ ; \*\*,  $P < 0.01$  compared with *Apoe*<sup>-/-</sup> using Student's unpaired *t* test ( $n = 4-8$ ).

### Quantification of atherosclerotic lesion size

The brachiocephalic artery was dissected out to provide a Y-shaped piece of vessel containing the origins of the subclavian and carotid arteries; this was embedded in paraffin. Serial sections (3  $\mu\text{m}$ ) were taken from the proximal 60  $\mu\text{m}$  of the brachiocephalic artery once the leaflets of the aortic arch were no longer visible. Sections were stained with US trichrome (UST); plaque sizes were quantified by light microscopy (Zeiss Axioskop; magnification,  $\times 10$ ; Zeiss, Oberkochen, Germany) with computerized planimetry (MCID Basic 7.0 image analysis soft-

ware; Imaging Research, Inc., Brock University, St. Catherines, Ontario, Canada). The area inside the internal elastic lamina was subtracted from the area inside the external elastic lamina to provide a measure of media area. Subclavian arteries from randomly selected mice in the drug study were also paraffin embedded and sectioned as above for morphometric studies.

### Immunohistochemistry

Plaque collagen content was assessed by Picrosirius red staining and extracellular lipid content by quantification of the holes left behind during histological processing of UST-stained sections (18). Plaque macrophage and smooth muscle cell (SMC) content was assessed using Mac-2 (VHBIO, Gateshead, UK) and smooth muscle  $\alpha$ -actin (Sigma, Poole, UK) antibodies, respectively. Vascular cell adhesion molecule 1 (VCAM-1) (Cambridge Biosciences, Cambridge, UK) antibody was used to investigate adhesion molecule expression (for details, please see Supplemental data, published on The Endocrine Society's Journals Online web site at <http://endo.endojournals.org>). Staining was imaged using a light microscope (Zeiss Axioskop) coupled to a Photometrics CoolSnap camera (Tucson, AZ). Photoshop CS3 Extended software was used to quantify staining, and data are expressed as stained areas relative to total plaque size (percentage). A semiquantitative scoring method (carried out blind to genotype) was employed to assess VCAM-1 expression, where an arbitrary score of 0–4 was given to each section based on the percentage of the circumference of the specific endothelial staining.

### Cell culture

Mouse aortic endothelial cells (MAECs cell line) (19) were maintained in endothelial basal medium 2 (Lonza, Slough, UK) supplemented with 10% fetal calf serum and Pen/Strep. Cells were treated overnight in serum-free medium with one of the following: 10 ng/ml TNF- $\alpha$  (Santa Cruz Biotechnology, Inc., Santa Cruz, CA), 1 nM aldosterone in the presence/absence of 1  $\mu\text{M}$  spironolactone, 1 nM corticosterone in the presence/absence of 1  $\mu\text{M}$  glycyrrhetic acid, and 1  $\mu\text{M}$  spironolactone (all from Sigma). VCAM-1 expression was quantified by counting the number of positively stained cells per field (at magnification,  $\times 40$ ) in four separate fields for each treatment.

**TABLE 1.** Increased atherogenesis in *E/b2* mice

	3 months		6 months	
	<i>Apoe</i> <sup>-/-</sup> (4)	<i>E/b2</i> (8)	<i>Apoe</i> <sup>-/-</sup> (6)	<i>E/b2</i> (8)
Area inside EEL ( $\times 10^3 \mu\text{m}^2$ )	100 $\pm$ 18	243 $\pm$ 30 <sup>a</sup>	182 $\pm$ 24	352 $\pm$ 27 <sup>b</sup>
Medial area ( $\times 10^3 \mu\text{m}^2$ )	39.6 $\pm$ 9.1	100.2 $\pm$ 10.4 <sup>b</sup>	53 $\pm$ 7.3	110 $\pm$ 5.4 <sup>b</sup>
Lesion area ( $\times 10^3 \mu\text{m}^2$ )	1.4 $\pm$ 1.4	48.1 $\pm$ 13.9 <sup>a</sup>	8.3 $\pm$ 7.1	151.0 $\pm$ 15.8 <sup>b</sup>
Lumen area ( $\times 10^3 \mu\text{m}^2$ )	59.0 $\pm$ 10.0	95.0 $\pm$ 12.0	127 $\pm$ 15.2	90.0 $\pm$ 16
Buried caps	0	0	0	1.86 $\pm$ 0.24 <sup>b</sup>
Macrophages % plaque area	0 (no plaques)	13.9 $\pm$ 5.2 (4)	7.7 $\pm$ 2.4 (4)	22.5 $\pm$ 2.1 (5) <sup>b</sup>

Histological analysis of brachiocephalic arteries identified extensive atherosclerotic lesions in 3-month-old *E/b2* mice but not in age-matched *Apoe*<sup>-/-</sup> mice. At 6 months of age, lesion size remained significantly increased in *E/b2* compared with *Apoe*<sup>-/-</sup> mice. The differences in lesion size were significant whether expressed as  $\text{mm}^2$  or as a percentage of the lesion area (lesion/area inside the external elastic lamina  $\times 100$ ) (Fig. 1). Increased lesion development in *E/b2* mice reduced the percentage luminal area (lumen/lumen + lesion area  $\times 100$ ), compared with *Apoe*<sup>-/-</sup> mice at both 3 and 6 months of age (Fig. 1). Absolute lumen area ( $\text{mm}^2$ ) was not reduced in *E/b2* mice due to extensive outward remodeling of the vessel (indicated by increased total area within the external elastic lamina). Buried fibrous caps were evident only in 6-month-old *E/b2* mice. These may be an indication of lesion 'vulnerability.' Data are mean  $\pm$  SEM, with group sizes shown in parentheses (*n*). EEL, External elastic lamina.

<sup>a</sup>  $P < 0.05$ .

<sup>b</sup>  $P < 0.01$  compared to age-matched *Apoe*<sup>-/-</sup> mice (Student's unpaired *t* test).

## Plasma lipid and lipoprotein analysis

Terminal blood samples were taken for lipid analysis from the left ventricle of vehicle- and drug-treated E/b2 and *ApoE*<sup>-/-</sup> mice. Total plasma cholesterol was measured by a

colorimetric reaction using the Cholesterol/Cholesteryl Ester Quantification kit (Merck, Whitehouse Station, NJ).

## Statistical analyses

Data were analyzed by the GraphPad Prism analysis package (GraphPad, San Diego, CA). Data are expressed as means  $\pm$  SEM. For analysis of unpaired datasets, Student's unpaired *t* test was used for comparison of two groups, and one-way ANOVA with Tukey's *post hoc* test was used for more than two groups. Repeated measures ANOVA was used for comparison of matched datasets. Two-way ANOVA followed by Bonferroni *post hoc* tests was used for analyzing the effects of drug treatments between groups. Scored data were analyzed by a nonparametric Kruskal-Wallis one-way ANOVA followed by Dunn's *post hoc* test. A *P* value of less than 0.05 was considered to be statistically significant.

## Results

### E/b2 mice show accelerated atherosclerosis

E/b2 mice were born in the expected Mendelian numbers to *ApoE*<sup>-/-</sup> *Hsd11b2*<sup>+/-</sup> females mated with E/b2 males and showed no difference in weight gain to *ApoE*<sup>-/-</sup> *Hsd11b2*<sup>+/-</sup> littermates or age-matched *ApoE*<sup>-/-</sup> mice.

At 3 months of age, *ApoE*<sup>-/-</sup> mice raised on a standard chow diet displayed few, if any, signs of atherosclerosis in the brachiocephalic artery (Fig. 1A). In contrast, by 3 months of age on the same diet, E/b2 mice lacking both 11 $\beta$ -HSD2 and ApoE displayed atheroma (lipid core and proliferating SMCs) with occasional thin fibrous caps, affecting the aortic arch and its major branches, including the brachiocephalic trunk (Fig. 1A), a site particularly susceptible to plaque development in these animals when fed an atherogenic "Western" diet (20). At 3 months, some severe lesions were already present in E/b2 mice, with extended necrotic areas, cholesterol clefts, neointimal expansion, and elastic lamina remodeling.

By 6 months of age, E/b2 mice displayed complex severe atherosclerotic

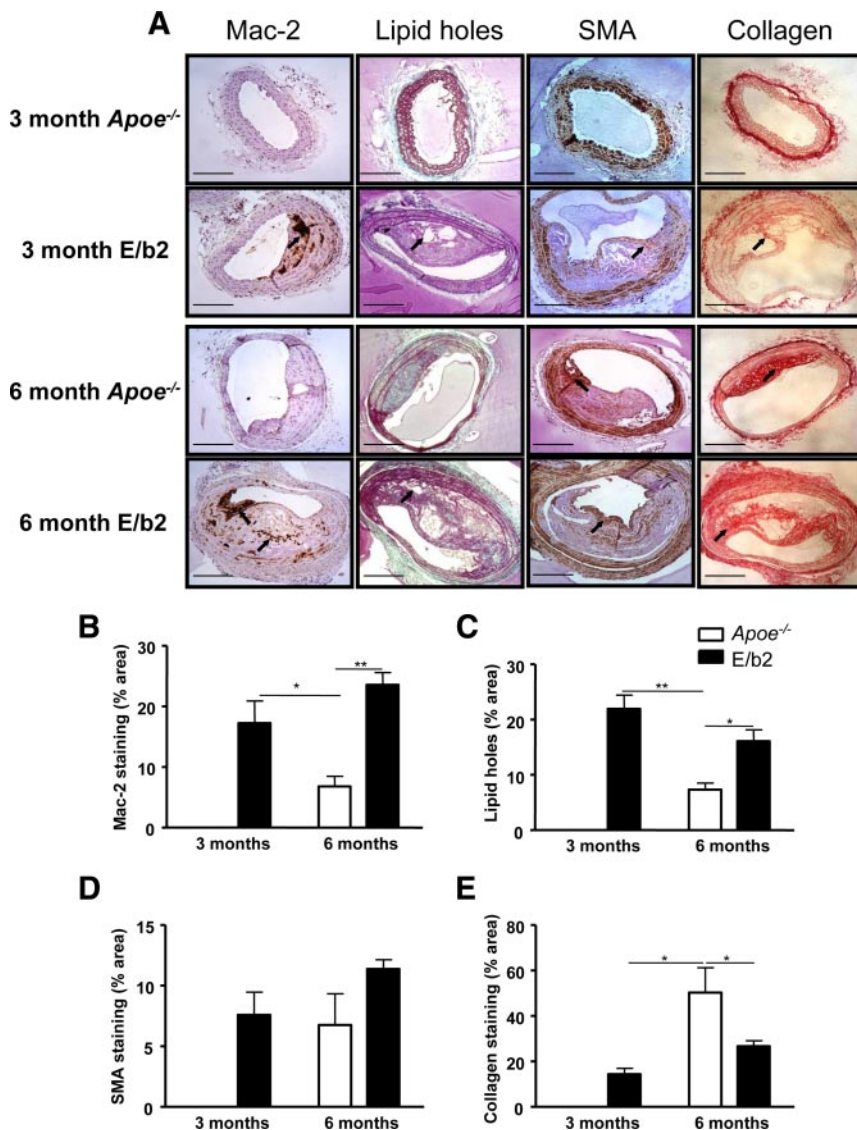


**FIG. 2.** Accelerated atherosclerosis in E/b2 mice is associated with macrophage infiltration and altered plaque composition. **A**, At 3 months of age, *ApoE*<sup>-/-</sup> mice are lesion free, whereas E/b2 mice show macrophage-infiltrated plaques (staining with anti-Mac-2 antibodies) with a high lipid and low collagen content. By 6 months, E/b2 mice have large macrophage-rich plaques with a high density of lipids and sparse collagen staining. In comparison, 6-month-old *ApoE*<sup>-/-</sup> mice have plaques that are rich in collagen and low in lipid and macrophage content. E/b2 and *ApoE*<sup>-/-</sup> mice at both ages show similar levels of  $\alpha$ -SMA staining, indicative of SMC within their plaques. Representative images (of six mice per group, except in case of 6-month-old *ApoE*<sup>-/-</sup>, where uncommon larger plaques were selected to investigate composition) captured at magnification,  $\times 10$ . Arrows indicate regions of interest corresponding to names of each column. Scale bar, 250  $\mu$ m. **B–E**, The area of staining for each plaque component was quantified using Photoshop CS3 Extended software and expressed as a percentage of total plaque area. Macrophage (B) and lipid (C) contents were both increased in brachiocephalic plaques from 3- and 6-month-old E/b2 mice compared with those from *ApoE*<sup>-/-</sup> mice at 6 months of age. There was no difference in the  $\alpha$ -SMA (D) content of plaques between *ApoE*<sup>-/-</sup> and E/b2 mice at either 3 or 6 months of age. Collagen (E) content was reduced in brachiocephalic plaques from 3- and 6-month E/b2 mice compared with those from *ApoE*<sup>-/-</sup> mice at 6 months of age. Data are mean  $\pm$  SEM, *n* = 5–7/group. Analyzed by two-way ANOVA; \*, *P* < 0.05; \*\*, *P* < 0.005.

lesions with multiple fibrous caps (Fig. 1B). Importantly, these included buried caps, which have been suggested as being indicative of earlier plaque instability (Fig. 1B and Table 1) (21). However, in 6-month-old *Apoe*<sup>-/-</sup> mice raised on the same chow diet, atherosclerosis remained sporadic (only one of the six animals in this group had a notable plaque; example shown in Fig. 1B) in the brachiocephalic artery (Fig. 1B). This remarkable increase in atherosclerosis with 11 $\beta$ -HSD2 deficiency was despite similar plasma cholesterol levels between E/b2 (306  $\pm$  54 mg/dl) and *Apoe*<sup>-/-</sup> (288  $\pm$  46 mg/dl) mice.

Quantitative analysis of the areas inside the external elastic lamina, lesion areas, and lumen areas of the brachiocephalic artery revealed significantly larger atherosclerotic lesions in E/b2 mice at 3 and 6 months of age compared with age-matched *Apoe*<sup>-/-</sup> mice (Fig. 1C and Table 1). There was also a significant reduction of lumen size relative to the size of the vessel (Fig. 1C and Table 1), although the absolute lumen size was maintained (vessel diameter was also increased), suggestive of expansive remodeling in E/b2 mice.

### Plaque composition is altered in E/b2 mice

Immunohistochemical staining revealed that atherosclerotic plaques in brachiocephalic arteries of 6-month-old E/b2 mice contained dense accumulations of macrophages and foam cells (Fig. 2A), most notably at the “shoulder” of lesions and near buried fibrous caps. Macrophage infiltration (Fig. 2B), and lipid content of plaques (Fig. 2C) were both significantly greater in E/b2 than in *Apoe*<sup>-/-</sup> mice. Furthermore, plaques in 3-month-old E/b2 mice contained significantly more macrophages (Fig. 2B) and lipid (Fig. 2C) than those in plaque size-matched *Apoe*<sup>-/-</sup> counterparts (examples of rare plaques from 6-month-old *Apoe*<sup>-/-</sup> mice selected to show composition). SMC content of plaques, assessed by  $\alpha$ -smooth muscle actin (SMA) immunoreactivity, did not differ between E/b2 and *Apoe*<sup>-/-</sup> mice (Fig. 2D). Picrosirius red staining of collagen was significantly lower in plaques from 3- and 6-month-old E/b2 mice compared with plaques from 6-month-old *Apoe*<sup>-/-</sup> mice (Fig. 2E). Thus, 11 $\beta$ -HSD2 deficiency promotes the formation of collagen-poor, lipid-, and macrophage-rich plaques, suggestive of a “vulnerable” plaque phenotype.

### Accelerated atherosclerosis in E/b2 mice is associated with increased expression of VCAM-1

VCAM-1 immunoreactivity was significantly higher in unaffected areas of brachiocephalic artery endothelium in both 3- and 6-month-old E/b2 mice compared with age-

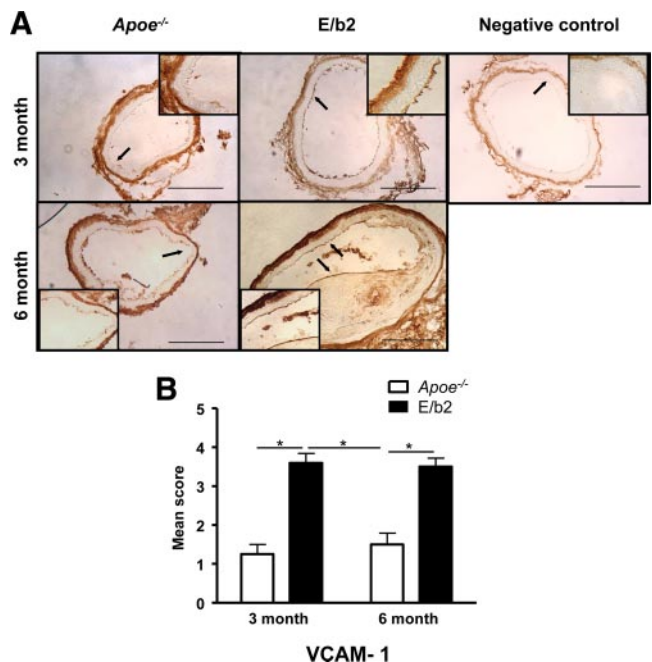


**FIG. 3.** Endothelial cell expression of VCAM-1 is up-regulated in E/b2 mice. *A*, *Apoe*<sup>-/-</sup> mice at 3 months show sparse endothelial staining for VCAM-1 (top left panel), whereas age-matched E/b2 mice have more abundant and intense VCAM-1 immunoreactivity (top middle panel). At 6 months, *Apoe*<sup>-/-</sup> mice (bottom left panel) show increased VCAM-1 staining compared with 3-month-old *Apoe*<sup>-/-</sup> mice, but it is still lower than in E/b2 mice (bottom right panel). Arrows indicate specific staining for VCAM-1 in endothelium (highlighted in embedded boxes). Adventitia is stained nonspecifically as a result of entrapment of streptavidin-horseradish peroxidase complex (see negative control). Representative images (of four to six mice per group) captured at magnification,  $\times 10$ . Scale bar, 250  $\mu$ m. *B*, VCAM-1 staining is significantly greater in endothelium of 3- and 6-month-old E/b2 mice compared with age-matched *Apoe*<sup>-/-</sup> mice. At 3 months, VCAM-1 expression is higher in E/b2 vessels compared with *Apoe*<sup>-/-</sup> mice at 6 months with the same size of plaques. Data are means  $\pm$  SEM,  $n = 4$ –6/group. Analyzed by Kruskal-Wallis nonparametric test; \*\*\*,  $P < 0.0001$ . Scoring: 0, absent; 1, <25% circumference stained; 2, 25–50% circumference stained; 3, 50–75% circumference stained; 4, >75% circumference stained.

matched *Apoe*<sup>-/-</sup> controls (Fig. 3) both in the endothelium covering the plaque and in plaque-free regions of the vessel wall. Importantly, comparison of similar-sized vessels from 3-month-old E/b2 mice and 6-month-old *Apoe*<sup>-/-</sup> mice showed significantly higher VCAM-1 expression in E/b2 mice, despite their younger age (Fig. 3, A and B).

### Atheroprotective effects of eplerenone and amiloride do not correlate with their ability to lower blood pressure

As anticipated from the previously reported phenotype of *Hsd11b2*<sup>-/-</sup> mice (9), E/b2 animals were moderately hypertensive compared with *Apoe*<sup>-/-</sup> mice, most likely due to overactivation of MR in the kidney (SBP 141.8  $\pm$  2.5 mm Hg in E/b2 mice vs. 112.6  $\pm$  1.7 mm Hg in *Apoe*<sup>-/-</sup> mice;  $P < 0.001$ ). Thus, the exacerbated athero-

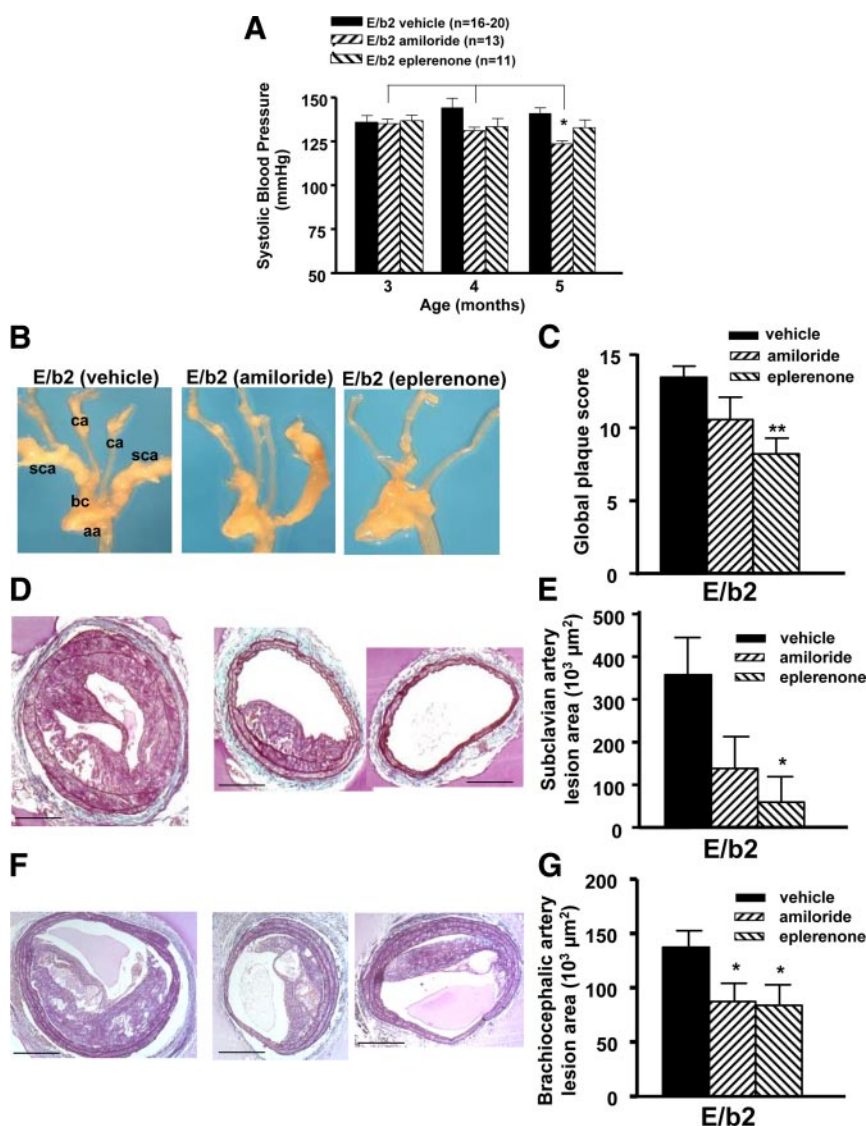


**FIG. 4.** Eplerenone reduces lesion size in E/b2 mice, independently of blood pressure. **A**, SBP in E/b2 and *Apoe*<sup>-/-</sup> mice was reduced in E/b2 mice by treatment with amiloride but not by eplerenone. \*,  $P < 0.05$  vs. age 3 and 4 months, repeated measures ANOVA. **B**, Representative images of the aortic arch and its branches in 5-month-old E/b2 mice after vehicle (*left panel*), amiloride (*center panel*), or eplerenone (*right panel*) treatment. aa, Aortic arch; ca, carotid artery; sca, subclavian artery; bc, brachiocephalic artery. **C**, Semiquantitative analysis of lesion development using global plaque score (for details, please see *Materials and Methods*). \*\*,  $P < 0.01$  vs. untreated E/b2 Kruskal-Wallis test,  $n = 6-11$ . **D**, Representative images of UST-stained plaques in subclavian arteries of 5-month-old E/b2 mice after vehicle (*left panel*), amiloride (*center panel*), and eplerenone (*right panel*) treatment. Images captured at magnification,  $\times 10$ . Scale bar, 250  $\mu\text{m}$ . **E**, Measurement of lesion size; \*,  $P < 0.05$  vs. untreated E/b2 mice, one-way ANOVA,  $n = 4-5$ . **F**, Representative images of UST-stained plaques in brachiocephalic arteries of E/b2 mice after vehicle (*left panel*), amiloride (*center panel*), and eplerenone (*right panel*) treatment. Images captured at magnification,  $\times 10$ . Scale bar, 250  $\mu\text{m}$ . **G**, Measurement of lesion size; \*,  $P < 0.05$  vs. untreated E/b2; two-way ANOVA,  $n = 7-10$ .

sclerosis in E/b2 mice could be attributable to hypertension as a result of renal MR activation by glucocorticoids, or to a direct effect of 11 $\beta$ -HSD2-deficiency within the vascular wall or a combination of these factors. To address MR involvement and to determine the dependency of the phenotype on hypertension, 2-month-old mice were fed chow diet containing vehicle or one of two pharmacologic

inhibitors for 3 months: amiloride, an ENaC blocker that acts downstream of renal MR to lower blood pressure, and eplerenone, a highly selective MR antagonist. The dose chosen for the latter (200 mg/kg  $\cdot$  d in chow) was previously shown to reduce atheroma formation in *Apoe*<sup>-/-</sup> mice administered aldosterone (22). We found no effect of any drug treatment on blood pressure of *Apoe*<sup>-/-</sup> mice (data not shown). Eplerenone had no significant effect on SBP in E/b2 mice, whereas amiloride reduced it by approximately 11 mm Hg, almost halving the blood pressure difference between E/b2 and *Apoe*<sup>-/-</sup> mice (Fig. 4A). However, despite being less effective as a hypotensive drug, eplerenone was more effective than amiloride in reducing overall plaque score as estimated by blinded, semi-quantitative scoring assessed across five sites (Fig. 4, B and C). Quantitative histological analysis showed that eplerenone also dramatically reduced plaque size and the expansive remodeling in subclavian arteries, which are particularly prone to large occlusive plaques in E/b2 mice (Fig. 4, D and E). Both eplerenone and amiloride reduced lesion size in brachiocephalic arteries (Fig. 4, F and G, and Table 2). The pattern of expansive remodeling evident in untreated E/b2 mice was also reduced after treatment with both eplerenone and amiloride (Table 2). Thus, the stronger atheroprotective effect of eplerenone in comparison with amiloride, with the latter producing a larger reduction in blood pressure, indicates that the predominant mechanism leading to accelerated atherosclerosis in E/b2 mice is unlikely to be attributable simply to hypertension after renal MR activation.

#### MR activation contributes to the altered plaque composition in E/b2 mice

To investigate whether MR antagonism altered plaque composition in addition to reducing lesion size in E/b2 mice, macrophage infiltration,  $\alpha$ -SMA, collagen, and lipid content were measured in brachiocephalic plaques of E/b2

**TABLE 2.** Histological analysis of the effect of treatment with amiloride or eplerenone on atherosclerotic lesion development in the brachiocephalic artery of E/b2 mice and *Apoe*<sup>-/-</sup> mice

	E/b2			
	Vehicle (10)	Amiloride (7)	Eplerenone (9)	<i>Apoe</i> <sup>-/-</sup> vehicle (10)
Area inside EEL ( $\times 10^3 \mu\text{m}^2$ )	400 $\pm$ 25.0 <sup>c</sup>	321 $\pm$ 27.2 <sup>a</sup>	304 $\pm$ 33.8 <sup>b</sup>	177 $\pm$ 9
Medial area ( $\times 10^3 \mu\text{m}^2$ )	119 $\pm$ 8.6 <sup>c</sup>	96.8 $\pm$ 5.0	89.6 $\pm$ 8.7 <sup>b</sup>	51.4 $\pm$ 3.7
Lesion area ( $\times 10^3 \mu\text{m}^2$ )	137 $\pm$ 15.4 <sup>c</sup>	87.2 $\pm$ 17.2 <sup>a</sup>	83.9 $\pm$ 19.1 <sup>b</sup>	5.8 $\pm$ 3.9
Lumen area ( $\times 10^3 \mu\text{m}^2$ )	144.4 $\pm$ 9.7	137.6 $\pm$ 19.8	130.5 $\pm$ 10.4	119.7 $\pm$ 6.7
Buried caps	1.1 $\pm$ 0.31	0.86 $\pm$ 0.26	0.56 $\pm$ 0.18	0

Vehicle-treated E/b2 mice demonstrated significant remodeling and atherosclerotic lesion formation compared with vehicle-treated *Apoe*<sup>-/-</sup> mice. Treatment of E/b2 mice with either amiloride or eplerenone significantly reduced the degree of vascular remodeling and atherosclerotic lesion formation in this vascular bed. Data are mean  $\pm$  SEM, with group sizes shown in parentheses (n). EEL, External elastic lamina.

<sup>a</sup>  $P < 0.05$ .

<sup>b</sup>  $P < 0.01$  when compared with vehicle-treated E/b2 mice, two-way ANOVA.

<sup>c</sup>  $P < 0.001$ , genotype comparison by Student's unpaired *t* test.

mice after 3 months of treatment with eplerenone or vehicle. Macrophage content was significantly reduced by eplerenone treatment (Fig. 5, A and B). Despite the increase in lipid content of plaques in E/b2 mice compared with *Apoe*<sup>-/-</sup> mice, MR blockade with eplerenone had no effect on plaque lipid content in E/b2 mice (Fig. 5, A and C). Surprisingly, although there was no difference in plaque  $\alpha$ -SMA content between E/b2 and *Apoe*<sup>-/-</sup> mice, SMC content was significantly increased by MR blockade in E/b2 mice (Fig. 5, A and D). Eplerenone treatment also significantly increased plaque collagen content compared with vehicle-treated E/b2 mice (Fig. 5, A and E). There was a trend toward a reduction in the incidence of buried fibrous caps in the brachiocephalic artery of eplerenone-treated E/b2 mice (1.10  $\pm$  0.31 buried caps for vehicle-treated mice *vs.* 0.56  $\pm$  0.18 for eplerenone-treated E/b2 mice).

### Glucocorticoids in the presence of 11 $\beta$ -HSD2 inhibitor cause MR-mediated up-regulation of VCAM-1 expression *in vitro*

MAECs were used to test whether mineralocorticoids or glucocorticoids acting through MR can affect VCAM-1 expression and whether 11 $\beta$ -HSD2 inhibition may be important in regulation of MR specificity. Similar to TNF- $\alpha$ , which potently increases VCAM-1 expression in endothelial cells (23), aldosterone markedly increased the number of MAEC expressing VCAM-1 (>7-fold) (Fig. 6), an effect blocked by pretreatment with the MR antagonist, spironolactone, suggesting an MR-mediated mechanism. Corticosterone alone had no effect on VCAM-1 expression. However, inhibition of 11 $\beta$ -HSD2 by pretreatment with glycyrrhetic acid [a widely used 11 $\beta$ -HSD inhibitor (24), which had no effect on VCAM-1 expression on its own] allowed corticosterone to induce a more than 9-fold increase in the number of VCAM-1-stained cells (Fig. 6). Using RT-PCR, we have confirmed that 11 $\beta$ -HSD1 is not

expressed in MAEC (data not shown). Thus, in this cell line, as in kidney, 11 $\beta$ -HSD2 protects MR from activation by glucocorticoids. Consistent with MR involvement, VCAM-1 up-regulation by corticosterone in the presence of glycyrrhetic acid was reversed by blockade of MR with spironolactone (Fig. 6B).

## Discussion

Early development of severe occlusive atheromatous plaques in E/b2 mice provides a new experimental model of atherosclerosis, mechanistically underpinned by glucocorticoid-mediated activation of MR. In contrast to most existing models, high fat/Western diet is not required for the development of atherosclerosis in E/b2 mice. Indeed, when fed a chow diet, *Apoe*<sup>-/-</sup> mice exhibit moderate hyperlipidemia and only develop mature atheromatous plaques at 8–10 months of age (25). Feeding *Apoe*<sup>-/-</sup> mice a Western diet (containing cholesterol) increases plasma cholesterol, induces systemic inflammation, and accelerates atherogenesis so that lesions appear within 5 wk (20). It therefore appears that progressive atherosclerosis in *Apoe*<sup>-/-</sup> mice is strictly dependent on systemic inflammation and elevated plasma cholesterol associated with the Western diet.

Atherogenesis in E/b2 mice was associated with early and increased macrophage infiltration of brachiocephalic lesions, even when matched with similar-sized lesions in older *Apoe*<sup>-/-</sup> mice. An increase in the number of buried caps in plaques of older E/b2 animals could reflect multiple events of plaque rupture and repair in E/b2 mice, typical of vulnerable plaques. Thus, for investigation of the processes leading to a vulnerable plaque phenotype, E/b2 mice may be a better experimental platform than *Apoe*<sup>-/-</sup> mice.

The ability of eplerenone administration to reduce plaque size and alter plaque composition implicates MR

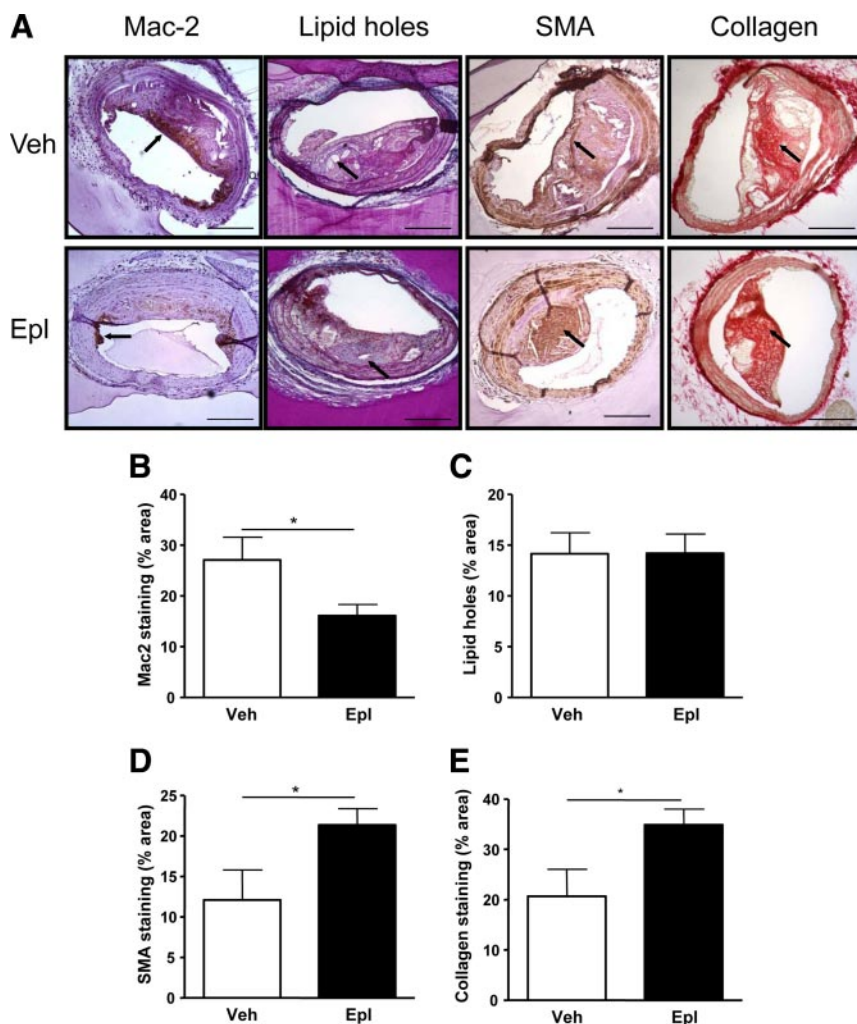


**FIG. 5.** MR blockade reduces macrophage infiltration and alters plaque composition in E/b2 mice. A, Representative images of atherosclerotic plaques from vehicle-treated (Veh) (top panels) and eplerenone-treated (Epl) (200 mg/kg · d; lower panels) E/b2 mice, stained with UST (lipid holes), Mac-2 antibody (Mac-2),  $\alpha$ -SMA antibody (SMA), or Picrosirius red (collagen), captured at magnification,  $\times 10$ . Arrows indicate regions of interest corresponding to names of each column. Scale bar, 250  $\mu$ m. Compared with vehicle-treated mice, plaques in eplerenone-treated E/b2 mice demonstrated reduced Mac-2 staining (B) with increased staining for  $\alpha$ -SMA (D) and collagen (E). There was no apparent difference in lipid content, compared with plaques in vehicle-treated E/b2 mice (C). The area of staining was quantified using Photoshop CS3 Extended software and expressed as a percentage of total plaque area. Data are mean  $\pm$  SEM,  $n = 4-5$ . Analyzed by Student's unpaired  $t$  test; \*,  $P < 0.05$ .

activation as mechanistically important in accelerating atherosclerosis in E/b2 mice. This is consistent with previous data showing that aldosterone is proatherogenic in animal models (23, 26), although this has not been replicated in all studies (27). Moreover, eplerenone has beneficial effects on experimental atherosclerosis in non-human primates (28), again implicating MR activation in pathogenesis of atherosclerosis. This raises the possibility that the proatherogenic effects of MR activation are through cortisol (a glucocorticoid) rather than the mineralocorticoid, aldosterone.

Crucially, the effect of eplerenone on atherosclerosis in E/b2 mice was independent of MR effects on blood pres-

sure (which was unaltered in E/b2 mice by this modest dose of eplerenone). In the absence of 11 $\beta$ -HSD2, MR are not protected from activation by glucocorticoids, and their activation in the distal nephron increases activity of ENaCs and Na/K ATPase, leading to hypertension (17). The extent of hypertension in E/b2 mice was comparable with that previously reported in single-knockout *Hsd11b2*<sup>-/-</sup> mice (9). Bypassing MR activation with the ENaC blocker amiloride reduced blood pressure in E/b2 mice but was less effective in diminishing atherosclerosis than eplerenone. Hypertension in *Hsd11b2*<sup>-/-</sup> mice is initiated by MR activation and volume expansion, but already after 2.5 months of age, activity of ENaC was returned to the basal level, and high blood pressure was maintained by activation of  $\alpha$  1-adrenergic receptors (26). Hence, eplerenone cannot effectively normalize blood pressure at these later stages, whereas amiloride still can. Another possible contributor to hypertension in *Hsd11b2* deficiency is the vasoconstrictive effect mediated by glucocorticoid receptors (29, 30), which will not be affected by the MR antagonist, eplerenone.

Thus, although hypertension may play a part in the accelerated atherogenesis in E/b2 mice, there is clearly a component of atherogenesis that is not merely due to the hypertension of “apparent mineralocorticoid excess” produced by MR overactivation in the distal nephron. This concurs with two previous studies in which blood pressure played little or no role in atherogenesis: in mice deficient for both ApoE and endothelial nitric oxide synthase (31) and *ApoE*<sup>-/-</sup> mice with renovascular hypertension (one kidney/one clip and two kidneys/two clips models) (32). In contrast, blood pressure *per se* played only a minor role in atheroma progression in *ApoE*<sup>-/-</sup> mice with renovascular hypertension compared with the large effect of angiotensin II (33).

Our data implicate activation of nonrenal MR in the pathogenesis of accelerated atherogenesis in E/b2 mice with the vascular wall being the most likely candidate site. In humans, 11 $\beta$ -HSD2 immunoreactivity has been re-

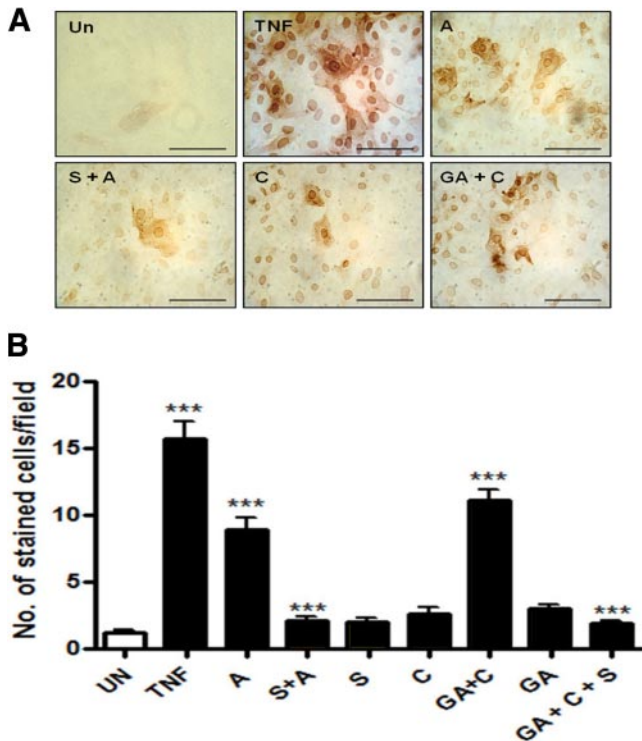


**FIG. 6.** VCAM-1 is induced after MR activation by glucocorticoids in MAECs. **A**, MAECs were treated for 24 h with 10 ng/ml TNF- $\alpha$ , 1 nM aldosterone (A), or 1 nM corticosterone (C), with or without pretreatment with 1  $\mu$ M spironolactone (S) or 1  $\mu$ M glycyrrhetic acid (GA) for 2 h before addition of aldosterone or corticosterone, as indicated. Un, Untreated cells. Brown staining shows VCAM-1 immunoreactivity. Images captured at magnification,  $\times 40$ . Scale bar, 250  $\mu$ m. **B**, VCAM-1 immunopositive cells were counted in four randomly selected fields (magnification,  $\times 40$ ) per treatment in five separate experiments. Data are mean  $\pm$  SEM of five experiments. Data were analyzed by one-way ANOVA; \*\*\*,  $P < 0.0001$ .

ported in arterioles and veins (34) with immunoreactivity and enzyme activity concentrated in endothelial cells (35). Both 11 $\beta$ -HSD2 mRNA and enzyme activity are found in rodent vessels, most likely including the endothelium (36). Consistent with colocalization of MR and 11 $\beta$ -HSD2 in endothelial cells, MAEC *in vitro* also have functional MR and 11 $\beta$ -HSD2. *In vitro*, activation of MR by aldosterone increases leukocyte adhesion molecules in primary human endothelial cells from umbilical cord (37). It was shown recently that aldosterone stimulates transcription of the proatherogenic leukocyte-endothelial cell adhesion proteins in human coronary artery and aortic endothelial cells. In the same study, inhibition of 11 $\beta$ -HSD2 enhanced cortisol-induced transcription of a reporter transgene mediated by MR in aortic endothelial cells (38). We show that VCAM-1 expression was increased *in vivo* in E/b2 mice in affected and unaffected regions of the brachiocephalic artery. A direct effect of MR in this increase (rather than an effect of shear stress) is supported by the MR-dependent potent increase in VCAM-1 expression in MAECs treated with aldosterone or with corticosterone in the presence of an

11 $\beta$ -HSD2 inhibitor. VCAM-1 increases monocyte/macrophage adhesion to endothelial cells (39) and is mechanistically linked to inflammatory processes (40) and atheroma development in *ApoE*<sup>-/-</sup> (41) and *Ldlr*<sup>-/-</sup> mice (42). Increased expression of VCAM-1 in E/b2 mice may be responsible for the increased macrophage infiltration leading to accelerated atherogenesis and may also stimulate expansive vessel remodeling (43).

Overall, these findings indicate that loss of function of 11 $\beta$ -HSD2 leads to striking atherogenesis in E/b2 mice mediated by activation of nonrenal MR. Endothelial expression of VCAM-1 and massive infiltration of the atherosclerotic plaques by macrophages at moderately elevated levels of plasma cholesterol are the characteristic features of this new mouse model of atherosclerosis.

We have shown for the first time that 11 $\beta$ -HSD2 is atheroprotective. In its absence, activation of MR mainly by glucocorticoids enhances inflammatory processes in the atherosclerotic plaque. This effect of MR is not solely attributable to changes in blood pressure. Whether it is associated with the altered activation mechanisms of MR in the endothelium remains to be investigated in the future experiments with tissue specific knockout of MR.

## Acknowledgments

We thank Dr. G. A. Gray for discussions and useful suggestions. Asim Azfer confirmed the absence of 11 $\beta$ -HSD1 mRNA in the MAEC cell line. Ms. Lorna Whiteside contributed to pilot work.

Address all correspondence and requests for reprints to: Yuri Kotelevtsev, Ph.D., Centre for Cardiovascular Science, The Queen's Medical Research Institute, 47 Little France Crescent, Edinburgh EH16 4TJ, United Kingdom. E-mail: ykotelev@staffmail.ed.ac.uk.

This work was supported the British Heart Foundation Project Grant PG/05/007/18240 [to Y.V.K. (principle investigator), G.A.D., P.W.F.H., J.R.S., D.G.B., and D.J.W.]. D.M. was the recipient of the Wellcome Trust Ph.D. Fellowship 078823/Z/05/Z. J.J.M. was the recipient of a Wellcome Trust Principal Research fellowship. D.J.W. was the recipient of a Wellcome Trust vacation scholarship.

Disclosure Summary: The authors have nothing to disclose.

## References

1. Pitt B, Zannad F, Remme WJ, Cody R, Castaigne A, Perez A, Palensky J, Wittes J 1999 The effect of spironolactone on morbidity and mortality in patients with severe heart failure. Randomized aldactone evaluation study investigators. *N Engl J Med* 341:709–717
2. Pitt B, Williams G, Remme W, Martinez F, Lopez-Sendon J, Zannad F, Neaton J, Roniker B, Hurley S, Burns D, Bittman R, Kleiman J 2001 The EPHEsus trial: eplerenone in patients with heart failure

- due to systolic dysfunction complicating acute myocardial infarction. Eplerenone post-AMI heart failure efficacy and survival study. *Cardiovasc Drugs Ther* 15:79–87
3. **Connell JM, Davies E** 2005 The new biology of aldosterone. *J Endocrinol* 186:1–20
  4. **Arriza JL, Weinberger C, Cerelli G, Glaser TM, Handelin BL, Housman DE, Evans RM** 1987 Cloning of human mineralocorticoid receptor complementary DNA: structural and functional kinship with the glucocorticoid receptor. *Science* 237:268–275
  5. **Walker BR** 2007 Glucocorticoids and cardiovascular disease. *Eur J Endocrinol* 157:545–559
  6. **Stewart PM, Corrie JE, Shackleton CH, Edwards CR** 1988 Syndrome of apparent mineralocorticoid excess. A defect in the cortisol-cortisone shuttle. *J Clin Invest* 82:340–349
  7. **Wilson RC, Krozowski ZS, Li K, Obeyesekere VR, Razzaghy-Azar M, Harbison MD, Wei JQ, Shackleton CH, Funder JW, New MI** 1995 A mutation in the HSD11B2 gene in a family with apparent mineralocorticoid excess. *J Clin Endocrinol Metab* 80:2263–2266
  8. **Edwards CR, Stewart PM, Burt D, Brett L, McIntyre MA, Sutanto WS, de Kloet ER, Monder C** 1988 Localisation of 11 $\beta$ -hydroxysteroid dehydrogenase—tissue specific protector of the mineralocorticoid receptor. *Lancet* 2:986–989
  9. **Kotelevtsev Y, Brown RW, Fleming S, Kenyon C, Edwards CR, Seckl JR, Mullins JJ** 1999 Hypertension in mice lacking 11 $\beta$ -hydroxysteroid dehydrogenase type 2. *J Clin Invest* 103:683–689
  10. **Fantidis P** 2010 The role of the stress-related anti-inflammatory hormones ACTH and cortisol in atherosclerosis. *Curr Vasc Pharmacol* 8:517–525
  11. **Walker BR** 2006 Cortisol—cause and cure for metabolic syndrome? *Diabet Med* 23:1281–1288
  12. **Takeda Y, Miyamori I, Yoneda T, Iki K, Hatakeyama H, Blair IA, Hsieh FY, Takeda R** 1995 Production of aldosterone in isolated rat blood vessels. *Hypertension* 25:170–173
  13. **Vicker N, Su X, Lawrence H, Cruttenden A, Purohit A, Reed MJ, Potter BV** 2004 A novel 18 $\beta$ -glycyrrhetic acid analogue as a potent and selective inhibitor of 11 $\beta$ -hydroxysteroid dehydrogenase 2. *Bioorg Med Chem Lett* 14:3263–3267
  14. **Nagasawa K, Chiba H, Fujita H, Kojima T, Saito T, Endo T, Sawada N** 2006 Possible involvement of gap junctions in the barrier function of tight junctions of brain and lung endothelial cells. *J Cell Physiol* 208:123–132
  15. **Zhang SH, Reddick RL, Piedrahita JA, Maeda N** 1992 Spontaneous hypercholesterolemia and arterial lesions in mice lacking apolipoprotein E. *Science* 258:468–471
  16. **Krege JH, Hodgin JB, Hagan JR, Smithies O** 1995 A noninvasive computerized tail-cuff system for measuring blood pressure in mice. *Hypertension* 25:1111–1115
  17. **Rossier BC, Pradervand S, Schild L, Hummler E** 2002 Epithelial sodium channel and the control of sodium balance: interaction between genetic and environmental factors. *Annu Rev Physiol* 64:877–897
  18. **Johnson J, Carson K, Williams H, Karanam S, Newby A, Angelini G, George S, Jackson C** 2005 Plaque rupture after short periods of fat feeding in the apolipoprotein E-knockout mouse: model characterization and effects of pravastatin treatment. *Circulation* 111:1422–1430
  19. **Nishiyama T, Mishima K, Ide F, Yamada K, Obara K, Sato A, Hitosugi N, Inoue H, Tsubota K, Saito I** 2007 Functional analysis of an established mouse vascular endothelial cell line. *J Vasc Res* 44:138–148
  20. **Nakashima Y, Plump AS, Raines EW, Breslow JL, Ross R** 1994 ApoE-deficient mice develop lesions of all phases of atherosclerosis throughout the arterial tree. *Arterioscler Thromb* 14:133–140
  21. **Williams H, Johnson JL, Carson KG, Jackson CL** 2002 Characteristics of intact and ruptured atherosclerotic plaques in brachiocephalic arteries of apolipoprotein E knockout mice. *Arterioscler Thromb Vasc Biol* 22:788–792
  22. **Keidar S, Kaplan M, Pavlotzky E, Coleman R, Hayek T, Hamoud S, Aviram M** 2004 Aldosterone administration to mice stimulates macrophage NADPH oxidase and increases atherosclerosis development: a possible role for angiotensin-converting enzyme and the receptors for angiotensin II and aldosterone. *Circulation* 109:2213–2220
  23. **Osborn L, Hession C, Tizard R, Vassallo C, Luhowskyj S, Chi-Rosso G, Lobb R** 1989 Direct expression cloning of vascular cell adhesion molecule 1, a cytokine-induced endothelial protein that binds to lymphocytes. *Cell* 59:1203–1211
  24. **Stewart PM, Krozowski ZS** 1999 11 $\beta$ -Hydroxysteroid dehydrogenase. *Vitam Horm* 57:249–324
  25. **Reddick RL, Zhang SH, Maeda N** 1994 Atherosclerosis in mice lacking apo E. Evaluation of lesional development and progression. *Arterioscler Thromb* 14:141–147
  26. **Bailey MA, Paterson JM, Hadoke PW, Wrobel N, Bellamy CO, Brownstein DG, Seckl JR, Mullins JJ** 2008 A switch in the mechanism of hypertension in the syndrome of apparent mineralocorticoid excess. *J Am Soc Nephrol* 19:47–58
  27. **Cassis LA, Helton MJ, Howatt DA, King VL, Daugherty A** 2005 Aldosterone does not mediate angiotensin II-induced atherosclerosis and abdominal aortic aneurysms. *Br J Pharmacol* 144:443–448
  28. **Takai S, Jin D, Muramatsu M, Kirimura K, Sakonjo H, Miyazaki M** 2005 Eplerenone inhibits atherosclerosis in nonhuman primates. *Hypertension* 46:1135–1139
  29. **Goodwin JE, Zhang J, Geller DS** 2008 A critical role for vascular smooth muscle in acute glucocorticoid-induced hypertension. *J Am Soc Nephrol* 19:1291–1299
  30. **Goodwin JE, Zhang J, Velazquez H, Geller DS** 2010 The glucocorticoid receptor in the distal nephron is not necessary for the development or maintenance of dexamethasone-induced hypertension. *Biochem Biophys Res Commun* 394:266–271
  31. **Chen J, Kuhlencordt PJ, Astern J, Gyurko R, Huang PL** 2001 Hypertension does not account for the accelerated atherosclerosis and development of aneurysms in male apolipoprotein e/endothelial nitric oxide synthase double knockout mice. *Circulation* 104:2391–2394
  32. **Mazzolai L, Korber M, Bouzourene K, Aubert JF, Nussberger J, Stamenkovic I, Hayoz D** 2006 Severe hyperlipidemia causes impaired renin-angiotensin system function in apolipoprotein E deficient mice. *Atherosclerosis* 186:86–91
  33. **Mazzolai L, Duchosal MA, Korber M, Bouzourene K, Aubert JF, Hao H, Vallet V, Brunner HR, Nussberger J, Gabbiani G, Hayoz D** 2004 Endogenous angiotensin II induces atherosclerotic plaque vulnerability and elicits a Th1 response in ApoE<sup>-/-</sup> mice. *Hypertension* 44:277–282
  34. **Smith RE, Little PJ, Maguire JA, Stein-Oakley AN, Krozowski ZS** 1996 Vascular localization of the 11 $\beta$ -hydroxysteroid dehydrogenase type II enzyme. *Clin Exp Pharmacol Physiol* 23:549–551
  35. **Jang C, Obeyesekere VR, Dilley RJ, Krozowski Z, Inder WJ, Alford FP** 2007 Altered activity of 11 $\beta$ -hydroxysteroid dehydrogenase types 1 and 2 in skeletal muscle confers metabolic protection in subjects with type 2 diabetes. *J Clin Endocrinol Metab* 92:3314–3320
  36. **Christy C, Hadoke PW, Paterson JM, Mullins JJ, Seckl JR, Walker BR** 2003 11 $\beta$ -Hydroxysteroid dehydrogenase type 2 in mouse aorta: localization and influence on response to glucocorticoids. *Hypertension* 42:580–587
  37. **Krug AW, Kopprasch S, Ziegler CG, Dippong S, Catar RA, Bornstein SR, Morawietz H, Gekle M** 2007 Aldosterone rapidly induces leukocyte adhesion to endothelial cells: a new link between aldosterone and arteriosclerosis? *Hypertension* 50:e156–e157
  38. **Caprio M, Newell BG, la Sala A, Baur W, Fabbri A, Rosano G, Mendelsohn ME, Jaffe IZ** 2008 Functional mineralocorticoid receptors in human vascular endothelial cells regulate intercellular adhesion molecule-1 expression and promote leukocyte adhesion. *Circ Res* 102:1359–1367

39. Ramos CL, Huo Y, Jung U, Ghosh S, Manka DR, Sarembock IJ, Ley K 1999 Direct demonstration of P-selectin- and VCAM-1-dependent mononuclear cell rolling in early atherosclerotic lesions of apolipoprotein E-deficient mice. *Circ Res* 84:1237–1244
40. Huo Y, Hafezi-Moghadam A, Ley K 2000 Role of vascular cell adhesion molecule-1 and fibronectin connecting segment-1 in monocyte rolling and adhesion on early atherosclerotic lesions. *Circ Res* 87:153–159
41. Dansky HM, Barlow CB, Lominska C, Sikes JL, Kao C, Weinsaft J, Cybulsky MI, Smith JD 2001 Adhesion of monocytes to arterial endothelium and initiation of atherosclerosis are critically dependent on vascular cell adhesion molecule-1 gene dosage. *Arterioscler Thromb Vasc Biol* 21:1662–1667
42. Cybulsky MI, Iiyama K, Li H, Zhu S, Chen M, Iiyama M, Davis V, Gutierrez-Ramos JC, Connelly PW, Milstone DS 2001 A major role for VCAM-1, but not ICAM-1, in early atherosclerosis. *J Clin Invest* 107:1255–1262
43. Brown NJ 2008 Aldosterone and vascular inflammation. *Hypertension* 51:161–167



Subscribe Now to a Valuable New CME Resource  
*Translational Endocrinology & Metabolism*  
Integrating Basic Science and Clinical Practice.

[www.endo-society.org](http://www.endo-society.org)